Photochemistry and Photobiology, 2000, 72(1): 146–150

Rapid Communication

In vivo Near-infrared Raman Spectroscopy: Demonstration of Feasibility During Clinical Gastrointestinal Endoscopy¶

Martin G. Shim[1], Louis-Michel Wong Kee Song[1,2], Norman E. Marcon[2] and Brian C. Wilson*[1]

[1]Department of Medical Biophysics, Ontario Cancer Institute/University Health Network, University of Toronto, Toronto, Ontario, Canada and
[2]Division of Gastroenterology, St. Michael's Hospital/Wellesley Central Site, University of Toronto, Toronto, Ontario, Canada

Received 13 April 2000; accepted 9 May 2000

ABSTRACT

Raman spectroscopy (RS) has potential for disease classification within the gastrointestinal tract (GI). A near-infrared (NIR) fiber-optic RS system has been developed previously. This study reports the first *in vivo* Raman spectra of human gastrointestinal tissues measured during routine clinical endoscopy. This was achieved by using this system with a fiber-optic probe that was passed through the endoscope instrument channel and placed in contact with the tissue surface. Spectra could be obtained with good signal-to-noise ratio in 5 s. The effects on the spectra of varying the pressure of the probe tip on the tissue and of the probe-tissue angle were determined and shown to be insignificant. The limited set of spectra from normal and diseased tissues revealed only subtle differences. Therefore, powerful spectral-sorting algorithms, successfully implemented in prior *ex vivo* studies, are required to realize the full diagnostic potential of RS for tissue classification in the GI.

INTRODUCTION

Endoscopy has altered the practice of gastroenterology by providing minimally invasive access to the gastrointestinal (GI)† tract. However, routine white-light endoscopy is insensitive in detecting micro-morphological and/or biochemical changes involving the mucosal lining of the GI tract (1–3). For instance, the detection of mucosal dysplasia (neoplastic epithelium) in patients with Barrett's esophagus (BE) or the differentiation of hyperplastic from neoplastic colon polyps routinely requires taking multiple biopsies for histopathological analysis. This approach results in significant costs for high-risk patients who require frequent surveillance in order to increase the chances of finding lesions at an early and curable stage. Recent developments in tissue spectroscopy may significantly expand our ability to diagnose GI diseases beyond the capabilities of standard white-light endoscopy by providing rapid tissue characterization *in situ*, thereby increasing the yield of tissue sampling, guiding biopsies of suspicious areas and reducing pathology costs and biopsy-associated risks.

Among the several optical methods currently under investigation for *in vivo* endoscopic applications, such as elastic scattering (4) and fluorescence (5) spectroscopy/imaging, Raman spectroscopy (RS) has the advantage of high molecular specificity, which may translate into more accurate tissue diagnosis. RS has shown promise in distinguishing between normal and diseased states of various organs including the skin, brain, breast, bladder, cervix, artery, colon and esophagus (6–8). However, the majority of this work has been done on *ex vivo* tissue specimens. In particular, to our knowledge, there have been no reports of RS used *in vivo* during routine clinical GI endoscopy.

In vivo RS is technically challenging due to the weak Raman signal of tissue, interference from tissue fluorescence and spectral contamination caused by the background Raman and fluorescence signals generated in the fiber-optic materials. We have developed a fiber-optic–based near-infrared (NIR) Raman system that is well suited for gastrointestinal endoscopic applications (9). This compact system incorporates filtered fiber-optic probes with "beam steering" technology, which suppresses the confounding background signals and optimizes the light collection efficiency (10). Herein, we demonstrate for the first time the feasibility of obtaining *in vivo* Raman spectra from various GI tract organs, with acceptable signal-to-noise ratio (SNR) and short collection times. This is a critical step prior to initiating systematic clinical trials to determine the diagnostic accuracy of the technique.

¶Posted on the web on 26 May 2000.
*To whom correspondence should be addressed at: Department of Medical Biophysics, Ontario Cancer Institute/University Health Network, 610 University Avenue, Rm 7417, Toronto, Ontario, M5G 2M9, Canada. Fax: 416-946-6529; e-mail: wilson@oci.utoronto.ca
†*Abbreviations:* BE, Barrett's esophagus; GI, gastrointestinal tract; NIR, near-infrared; (P)ANN, (probabilistic) artificial neural network; PCA, principal component analysis; RS, Raman spectroscopy; SNR, signal-to-noise ratio.

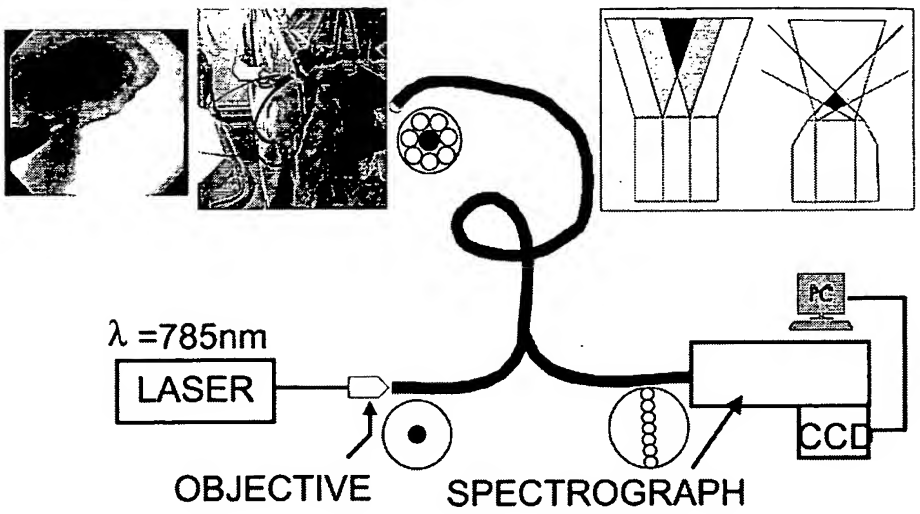

Figure 1. Schematic of the *in vivo* RS system and the probe tip. The probe is also shown being inserted into the instrument channel of an endoscope and in contact with a region of Barrett's mucosa in the esophagus. The insert illustrates the collection cones of a standard (left) fiber-optic probe and *in vivo* Raman probe. The shaded regions indicate the overlap of the illumination cone of the delivery fiber and the collection cones of the collection fibers.

MATERIALS AND METHODS

In vivo Raman system. The Raman instrument has been described previously (Fig. 1) (9). Briefly, it consists of a tunable laser diode (Model 8630, SDL, San Jose, CA) emitting at 785 nm and providing ~500 mW of excitation power, a high-throughput holographic spectrograph (Holospec f/1.8, Kaiser Optical Systems Inc., Ann Arbor, MI) and a liquid-N_2–cooled charge-coupled device detector array (Series 2000, Photometrics Ltd., Tucson, AZ). The instrument is mounted on a mobile cart, operates on standard electrical power and meets safety criteria for patient use. The spectral resolution using a 250 μm slit is 12 cm^{-1} and each pixel covered 2 cm^{-1}. For endoscopic applications, 3.0 m long bifurcated fiber-optic probes (Enviva Raman probes, Visionex, Inc., Atlanta, GA) were custom made (10). These comprise a central delivery fiber (400 μm core diameter), surrounded by seven collection fibers (300 μm core diameter). These reusable probes are intended for contact use and have a smooth 2 mm outer diameter tip that minimizes tissue trauma. Despite having a 1 cm long rigid tip, they pass easily through the accessory channel of a standard gastrointestinal endoscope. The probes incorporate longpass filters (0–80% transmission from 0–300 cm^{-1}) in the collection fibers and a bandpass filter (90% maximum transmission, 150 cm^{-1} full width at half maximum bandwidth) in the delivery fiber, that markedly reduce the confounding fluorescence and Raman background signal generated in the fiber optics. The collection fibers are cut at an angle and coated with a reflective surface to increase the overlap of the delivery and collection light cones in the tissue (Fig. 1, insert). This increases the signal-to-noise and limits the effective depth of tissue sampling to approximately 500 μm (10), so that the spectra correspond predominately to the mucosal layer of the GI tract, the critical layer for early-stage disease.

Endoscopic–spectroscopic procedure. Patients scheduled for either upper or lower GI endoscopy at St. Michael's Hospital/Wellesley Central Site were recruited. Ethical approval was obtained from the Institutional Review Board for all patients reported here and patients provided written informed consent.

Standard intravenous sedatives and analgesics were administered. Spectra were obtained from normal and/or diseased sites within the esophagus, stomach and colon, with the probe touching the mucosal surface with sufficient pressure to ensure that it remained stationary during each 5 s measurement. An incident power of 100 mW was used, and a shutter blocked the endoscope's white light during measurements. The probed site was then biopsied and the tissue samples were fixed in formalin for routine histopathology. Between patients, the probe was detached from the system for cleaning, soaked in 2% activated glutaraldehyde (Cidex, Johnson & Johnson, Arlington, TX), rinsed thoroughly with water and then swabbed with ethanol. At the time of writing, Raman spectra have been successfully collected from approximately 400 sites in 20 patients.

Spectral calibration and processing. Prior to use of the system with each patient, intensity and wavelength calibration was performed using a tungsten:halogen lamp, 4-acetamidophenol (A730-2, Aldrich, Milwaukee, WI) and polystyrene (18,243-5, Aldrich) calibration standards. This has been previously described in detail elsewhere (9). The broad background spectrum due to tissue autofluorescence and fiber-optic fluorescence was subtracted using a fifth-order polynomial fit to the intensity- and wavelength-corrected spectra to reveal the narrow Raman peaks from tissue.

Probe-tissue angle and pressure. The possibility of spectral artifacts caused by changes in probe pressure and angle on tissue were assessed in the stomach antrum, access to which permitted easy manipulation of the probe on the tissue surface. Three consecutive spectra (t = 5 s, P = 100 mW) were collected from the same site with mild, moderate and firm probe-tissue pressure, with a 10 s recovery period with the probe lifted from the tissue surface between measurements. Mild pressure corresponded to the probe just lightly touching the tissue surface, while firm pressure was enough to visibly indent the surface and cause some reduction in local blood content of the tissue. These spectra were collected *in vivo* and pressure variations were manually controlled by the endoscopist. Two different sites were scanned in three patients for a total of 18 spectra. In order to quantify these pressures, the probe was placed through an endoscope and placed in contact at 70°, relative to the tissue surface, with excised muscle tissue on a weighing balance. The endoscopist repeated each pressure measurement three times. These measurements were repeated three times. Spectra were also collected for probe-tissue angles of 70–90° (near perpendicular to tissue surface) and 10–20°, again with a 10 s recovery period, at three different sites in three patients for a total of 18 spectra. These spectra were analyzed with principal component analysis (PCA) and an artificial neural network (ANN) to determine if there were any systematic or significant differences due to pressure or angle. Principal components are a set of virtual spectra from which weighted linear combinations can generate any of the measured spectra within a specified % variance, typically 95% (11). The weights, also called scores, provide information about how the spectra are correlated. ANN are computer algorithms that are trained to associate input patterns (in this case the Raman spectra) with known output factors (here, the pathologic categories). The network then may be used to 'predict' the pathology from a new spectrum that was not in the training set (12). Spectra were calibrated and baseline subtracted as described previously and PCA was performed using the PLS Toolbox (Eigenvector Research, Inc., Manson, WA) in Matlab (The Mathworks, Natick, MA). For PCA, the calibrated spectra were normalized so that the mean spectrum was zero and the standard deviation unity. The entire spectral range (450–1800 cm^{-1}) was used and each spectrum was represented as a set of 1024 intensities (PCA variables). The ANN was a two-layer probabilistic artificial neural network (PANN) implemented in Matlab using the Neural Network

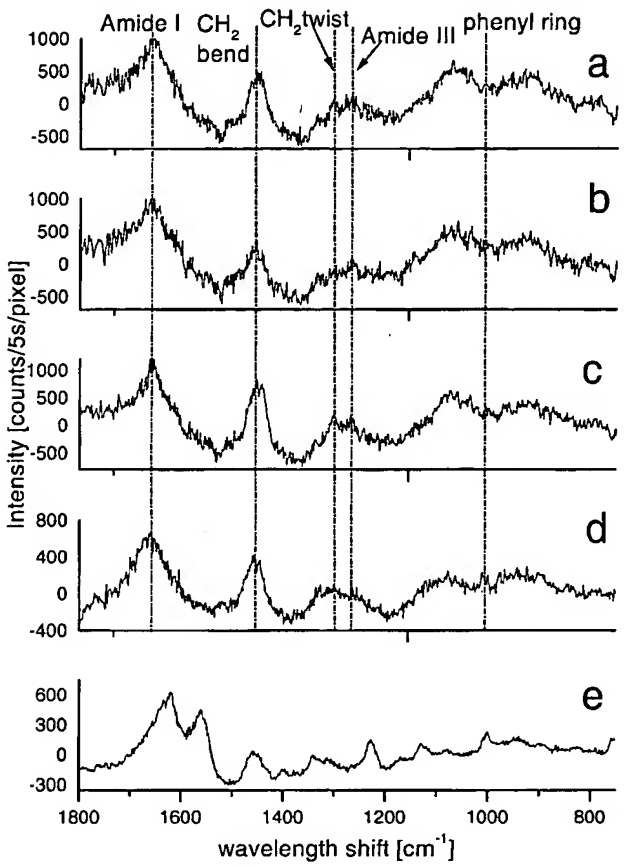

Figure 2. *In vivo* Raman spectra of human esophagus (t = 5 s, P = 100 mW, moderate pressure, 20° angle): (a) normal tissue; (b) Barrett's (intestinal metaplasia) without neoplastic transformation; (c) low-grade dysplasia (early neolpastic changes) in Barrett's; (d) high-grade dysplasia (progressive neoplastic changes) in Barrett's; and (e) pool of blood within the esophagus.

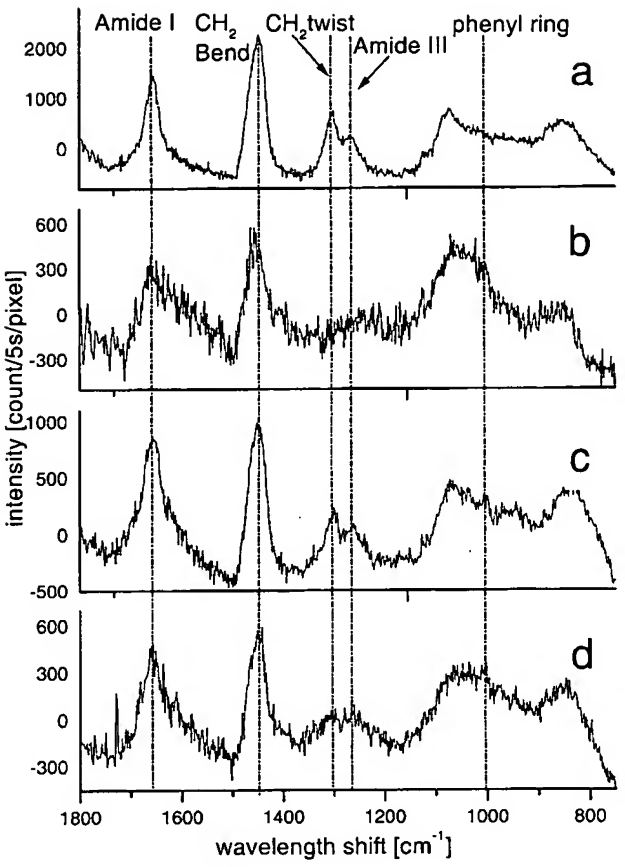

Figure 3. *In vivo* Raman spectra of human colon (t = 5 s, P = 100 mW, moderate pressure, 20° angle): (a) normal tissue; (b) hyperplastic polyp (benign); (c) adenomatous colon polyp (malignant potential); and (d) high-risk dysplasia-associated lesion or mass associated with chronic ulcerative colitis.

Toolbox (The Mathworks). The entire spectral range of the calibrated, baseline-subtracted spectra and their corresponding classifications (patient number, pressure or angle) were input as a training set. The objective was to compare the intrapatient variations due to pressure or angle with the interpatient variations. When a spectrum of unknown classification is input to the trained PANN, the first layer calculates a distance between the unknown spectrum and each of the spectra in the training set. The second layer uses these distances to calculate a set of probabilities that the unknown spectrum is a member of each of the possible classifications. The highest probability determines the final classification of the unknown spectrum.

RESULTS

Figures 2 and 3 show representative spectra of normal and abnormal regions in the esophagus and colon, respectively. SNR were calculated as the ratio of the absolute intensity above the baseline of the methyl bending mode at 1450 cm^{-1} *versus* the noise. Noise was defined as the absolute distance between the maximum and minimum intensity in the 1750–1800 cm^{-1} range. For esophagus, SNR are in the 3–5 range for normal and diseased tissues. The spectrum of normal colon was rich in lipid and the SNR is much higher (~17) relative to its diseased counterparts (4–8). Raman peaks below about 1100 cm^{-1} are difficult to interpret despite the use of the filtered probes, since narrow silica peaks persist, as seen for example at 850 cm^{-1} in Fig. 3. Typical tissue Raman bands are seen at 1655–1659, 1450–1453, 1310, 1260 and 1003 cm^{-1}, which can readily be assigned to the protein amide I band, CH_2 bending mode, CH_2 twisting mode, protein amide III band and the phenyl ring breathing mode, respectively (13).

During the collection of biopsies, small pools of blood routinely gather in the esophagus. The spectrum in Fig. 2e was collected from such a pool by holding the probe 1 mm above the blood. This spectrum is distinctive from tissue spectra and is characterized by heme vibrational modes at 1620, 1560, 1340, 1227 and 1128 cm^{-1}, in addition to the CH_2 bending mode at 1453 cm^{-1} and the phenyl ring breathing mode at 1000 cm^{-1} (14). The spectral features of heme did not contaminate the collection of Raman spectra from tissue amid pooling blood. This was confirmed when the probe was passed through the blood and placed in contact with the esophagus. The aforementioned heme peaks were absent, and the resultant tissue spectrum was confirmed to be normal esophagus.

For both the esophagus and colon, subtle differences in spectral lineshapes in the range 1100–1800 cm^{-1} are seen between normal and pathologic states, but no specific prom-

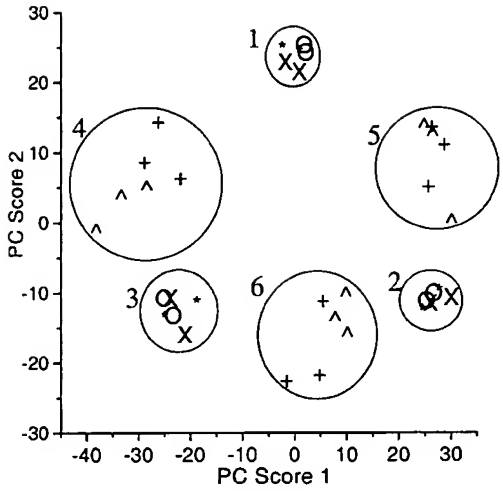

Figure 4. PCA scatter plot of score 1 *versus* 2. Spectra were collected from three patients (patients 1, 2 and 3) using mild (×), moderate (*) and firm (○) pressure. Spectra were also collected from three patients (patients 4, 5 and 6) with a 10–20° (^) and 70–90° (+) probe-tissue angle. The circles indicate the clustering of the data points for each patient.

inent changes in peak intensity or position are evident. We are currently investigating statistical/computational techniques such as PCA and ANN that utilize the complete spectrum for disease classification. Such algorithms will then be used prospectively to assess the accuracy of *in vivo* RS for GI diagnostics. Initial studies on spectra taken *ex vivo* on tissue biopies have been encouraging; for example, based on 260 samples from 17 BE patients, ANN could differentiate dysplasia from intestinal metaplasia (Barrett's) with a sensitivity of 77% and a specificity of 93% (15).

Measurements were taken to characterize the spectral artifacts caused by variation in probe-tissue pressure. The average mild, moderate and firm pressures (±1 standard deviation) measured *ex vivo* were 9.2 ± 2.4, 17.1 ± 1.7 and 31.1 ± 4.5 g mm^{-2}, respectively. Overall, no significant differences in spectra could be attributed to variations in probe pressure onto tissue. Some variation at 700–800 cm^{-1} and a baseline offset in the raw spectra (prior to polynomial subtraction) were observed in spectra collected at different pressures. Relative to the moderate tissue spectra, the offset at the middle of the tissue fingerprint region at 1300 cm^{-1} was in the 0–37% range. Positive and negative offsets did not consistently correspond to pressure, so that, for example, increased pressure did not always correspond to an increased offset. These apparently random spectral changes may have been due to differences in the fiber-optic background signal caused by small changes in probe bending which affect the coupling of Rayleigh scattered light into the probe. However, this needs to be confirmed. PCA analysis and an ANN were used to identify spectral variations due to pressure, which could have been missed by visual inspection. Figure 4 is a plot of the scores of the first and second principal components that captured 43 and 29% of the variation in the spectra, respectively. The spectra clustered into separate groups for each patient number, but did not separate within these clusters for different probe pressures. Similar results (data not shown) were observed for higher-order principal components that encompass approximately 95% of the spectral variance. Additional analysis is required before extensive evaluation of the diagnostic accuracy is performed. The observation that the spectra were consistent within each patient, but did not correlate to tissue-probe pressure, was supported by the ANN, as there was perfect correlation (18 of the 18 spectra correctly classified) between spectra and patient number. Conversely, 17 of the 18 spectra were misclassified to the wrong pressure classification indicating that there was no correlation between the two.

Upon visual inspection, no artifacts were identified in spectra collected at different probe-tissue angles. Difference spectra (not shown) calculated between spectra collected at 10–20° *versus* 70–90° were mostly noise. Baseline offsets at 1300 cm^{-1} of 2–50% were observed, the direction of which did not correspond to the angle used. This change in baseline is probably due to changes in the fiber-optic background signals that are sensitive to the probe bending used to change the probe-tissue angle. PCA scores 1 and 2 captured 58 and 15% of the spectral variance, respectively. The PCA plot of these scores (Fig. 4) revealed that spectra correlated well with patient number, but as indicated by their larger radii relative to the probe pressure measurements, there was more variation within these clusters. This is best seen for patient number 4 where there is a correlation of spectra with probe-tissue angle. This variation is probably due to the aforementioned changes in the fiber-optic background signal. The higher degree of correlation between the spectra and patient number relative to probe-tissue angle was also supported by the ANN where 18 of 18 spectra were correctly sorted by patient number, but only 7 of the 18 spectra were classified into the correct angle group.

DISCUSSION

As stated above, with the probes used here, it is estimated that the effective sampling depth is ~500 μm. This is an advantage for classifying early-stage lesions confined to the mucosa, since confounding signals originating from deeper layers are minimized. It fits well with the goal of endoscopic surveillance in BE or chronic ulcerative colitis patients, where detection of dysplasia before submucosal invasion provides an excellent chance for cure.

No significant artifacts could be attributed to blood. The ability to measure tissue spectra reliably even when the probe passes through a surface blood pool is reassuring, since the collection of spectra in a relatively bloody field is a likely scenario during endoscopic biopsy surveillance. Probe-tissue pressure and angle measurements showed that there were no specific major spectral artifacts caused by these factors during clinical use. PCA and ANN indicate that the main components contributing to tissue classification are insensitive to pressure changes, but perhaps more sensitive to the angle. However, it will be necessary to assess the effects on the PCA components that may be important for diagnostic accuracy. Changing the angle may also change the tissue volume or depth sampled, which could affect the diagnostic information obtained. Further studies are in progress.

The peristaltic movement of the GI tract prohibits accurate probe placement over a localized site for prolonged periods.

However, with occasional use of standard antiperistaltic drugs and moderate probe-tissue pressure, we experienced little difficulty in keeping the probe in position during the 5 s measurement time. This time was a good compromise between obtaining adequate SNR (SNR_{1450} = 3–17) and excessively extending endoscopy time and patient discomfort. It is anticipated that even shorter spectrum collection times can be achieved with technical improvements, such as systems with increased optical throughput and detectors with improved sensitivity. This would allow more sampling points and/or a reduction in procedure time. In addition to its diagnostic accuracy, these are important determinants of the overall cost-effectiveness of the technique in routine clinical practice.

With regards to safety, the NIR light is nonmutagenic. Recent tests on *ex vivo* esophageal tissue samples using an IR camera (16) show that 250 mW of 830 nm light focused to a 500 μm spot size does not produce detectable temperature increase (<0.8°) over an exposure time of greater than 1 min. Hence, 5 s exposures per point *in vivo* at 100 mW, over a comparable spot size, with a nearby NIR wavelength and with blood perfusion, should not result in thermal damage. Indeed, none was noted here on histological examination of the biopsies. With its smooth tip and size, the probe did not cause any visible trauma to the tissue in any patient, and of course, there is no electrical connection to the probe.

Raman spectra of calibration standards collected with probes that had undergone repeated gas sterilization (unpublished data) showed that this technique might be used for cleaning. We have not attempted autoclave sterilization of the probes, but it may also be possible to use a sterile sheath over the tip if necessary for other applications, providing the sheath does not contribute to the tissue Raman signal.

In conclusion, the development of a user-friendly, compact and portable Raman system complete with specialized fiber-optic probes has enabled, for the first time, *in vivo* RS to be performed noninvasively during routine clinical GI endoscopy, with acceptable SNR and measurement times. We believe that this is a significant step forward in optical diagnostics and have initiated systematic studies to determine the diagnostic accuracy and utility for a variety of preneoplastic and neoplastic gastrointestinal conditions. In addition, clinical trials are planned for several other non-GI sites, both for disease detection/differential diagnosis and for surgical/therapeutic guidance.

Acknowledgements—This project was funded by Photonics Research Ontario. L.-M.W.K.S. was supported by the Mayo Clinic and Foundation, Rochester, MN. We would like to thank Michael Wach and Eric Marple of Visionex, GA for their help in customizing the GI probe.

REFERENCES

1. Suvakovic, Z., M. G. Bramble, R. Jones, C. Wilson, N. Idle and J. Ryott (1997) Improving the detection rate of early gastric cancer requires more than open access gastroscopy: a five year study. *Gut* **41**, 308–313.
2. Robertson, C. S., J. F. Mayberry, D. A. Nicholson, P. D. James and M. Atkinson (1988) Value of endoscopic surveillance in the detection of neoplastic change in Barrett's oesophagus. *Br. J. Surg.* **75**, 760–763.
3. Levine, D. S., R. C. Haggitt, P. L. Blount, P. S. Rabinovitch, V. W. Rusch and B. J. Reid (1993) An endoscopic biopsy protocol can differentiate high-grade dysplasia from early adenocarcinoma in Barrett's esophagus. *Gastroenterology* **105**, 40–50.
4. Wallace, M. B. and J. Van Dam (2000) Enhanced gastrointestinal diagnosis: light-scattering spectroscopy and optical coherence tomography. *Gastrointest. Endosc. Clin. N. Am.* **10**, 71–80.
5. DaCosta, R. S., B. C. Wilson and N. E. Marcon (2000) Light-induced fluorescence endoscopy of the gastrointestinal tract. *Gastrointest. Endosc. Clin. N. Am.* **10**, 37–69.
6. Mahadevan-Jansen, A. and R. Richards-Kortum (1996) Raman spectroscopy for the detection of cancers and precancers. *J. Biomed. Opt.* **1**, 31–70.
7. Wolthuis, R., T. C. Bakker Schut, P. J. Caspers, H. P. J. Buschman, T. J. Romer, H. A. Bruining and G. J. Puppels (1999) Raman spectroscopic methods for *in vitro* and *in vivo* tissue characterization. In *Fluorescent and Luminescent Probes for Biological Activity: A Practical Guide to Technology for Quantitative Real-Time Analysis*, 2nd Ed. (Edited by W. T. Mason), pp. 433–455. Academic Press, Toronto.
8. Manoharan, R., K. Shafer, L. Perelman, J. Wu, K. Chen, G. Deinum, M. Fitzmaurice, J. Myles, J. Crowe, R. R. Dasari and M. S. Feld (1998) Raman spectroscopy and fluorescence photon migration for breast cancer diagnosis and imaging. *Photochem. Photobiol.* **67**, 15–22.
9. Shim, M. G. and B. C. Wilson (1997) Development of an *in vivo* Raman spectroscopic system for diagnostic applications. *J. Raman Spectrosc.* **28**, 131–142.
10. Shim, M. G., B. C. Wilson, E. Marple and M. Wach (1999) A study of fiber-optic probes for *in vivo* medical Raman spectroscopy. *Appl. Spectrosc.* **53**, 619–627.
11. Malinowski, E. R. (1991) *Factor Analysis in Chemistry*, 2nd Ed. Wiley, New York.
12. Lewis, I. R., N. W. Daniel Jr., N. C. Chaffin and P. R. Griffiths (1994) Raman spectrometry and neural networks for the classification of wood types-1. *Spectrochim. Acta* **50A**, 1943–1958.
13. Guan, Y., E. N. Lewis and I. W. Levin (1999) Biomedical applications of Raman spectroscopy: Tissue differentiation and potential clinical usage. In *Analytical Applications of Raman Spectroscopy* (Edited by M. J. Pelletier), pp. 276–327. Blackwell, Malden.
14. Ozaki, Y., A. Mizuno, H. Sato, K. Kawauchi and S. Muraishi (1992) Biomedical applications of near-infrared Fourier Transform Raman spectroscopy. Part I. The 1064-nm excited Raman spectra of blood and methemoglobin. *Appl. Spectrosc.* **46**, 533–536.
15. Shim, M. G., L.-M. Wong Kee Song, N. E. Marcon, S. Hassaram and B. C. Wilson (2000) Assessment of *ex vivo* and *in vivo* near-infrared Raman spectroscopy for the classification of dysplasia within Barrett's esophagus. *Proc. SPIE* (In press)
16. Puppels, G. J., T. C. Bakker Schut, P. J. Caspers, R. Wolthuis, M. G. Shim, H. A. Bruining and B. C. Wilson (2000) *In vivo* Raman spectroscopy. In *Handbook of Raman Spectroscopy* (Edited by I. R. Lewis and H. G. M. Edwards). Marcel Dekker, New York (in press)